Finite Elements in Analysis and Design 97 (2015) 1–19

Contents lists available at ScienceDirect

Finite Elements in Analysis and Design

journal homepage: www.elsevier.com/locate/finel

Calibration of the continuous surface cap model for concrete

Hua Jiang [a,b,*], Jidong Zhao [a]

[a] Dept of Civil and Environmental Engineering, the Hong Kong University of Science and Technology, Clearwater Bay, Kowloon, Hong Kong SAR, China
[b] Key Laboratory for Bridge and Tunnel of Shaanxi Province, Chang'an University, Xi'an, China

ARTICLE INFO

Available online 20 January 2015

Keywords:
Concrete
Constitutive model
Numerical simulation
LS-DYNA
MAT 145
MAT 159

ABSTRACT

The continuous surface cap (MAT 145) model in LS-DYNA is known by its elegant and robust theoretical basis and can well capture many important mechanical behaviors of concrete. However, it appears to be less popular than many other constitutive models in engineering application due to many material parameters involved in the model formulation which are difficult to calibrate. This study presents an effective calibration method to determine the material parameters for this model as functions of uniaxial compression strength and the maximum aggregate size of concrete according to formulas from CEB-FIP code and concrete test data from other published literatures. The obtained parameters can be conveniently used for occasional users with little or no information on concrete in hand. We further compare the predictions of stress–strain relationship in tension and compression under different confining pressures as well as hydrostatic compression by the model, and validate the model based on impact test of RC beams. Besides, the model is further compared against a similar model-MAT 159 in terms of model performance. The results demonstrate that the model based on the calibrated parameters is capable of offering reasonable and robust predictions.

1. Introduction

Arguably one of the most widely used man-made materials, concrete underpins the performance and safety for key structures relevant to civil engineering, onshore and offshore engineering, nuclear facility protection and many others. The dynamic responses of concrete when subjected to impact or blast loads are of particular importance in many of these engineering fields, and relevant research has hence attached much interest. Computer modeling has now been widely adopted as a cheap and effective way in assisting the design of (reinforced) concrete structures under those extreme loads. Among many key ingredients that affect reliable and accurate predictions by a numerical tool, an appropriately developed and calibrated constitutive model to describe the dynamic behavior of concrete subjected to dynamic loads plays a core role.

There have been a good number of constitutive models developed in the literature for concrete, with forms ranging from relatively simple to more sophisticated (see a recent review in [1,2]). They have also been implemented in commercial software such as LS-DYNA [3], AUTODYN [4] and ABAQUS/explicit [5]. These models can be generally divided into three categories according to how the plastic deformation is calculated. Category one normally adopts an associated flow to calculate the plastic strain increment, and may capture the plastic volume expansion (dilatancy) [6] caused by shear loading at low confining pressure. It considers coupled volumetric and shear behavior (i.e. shear enhanced compaction and pressure dependence of shear strain) of concrete. Typical examples of this category include the geologic cap (MAT 25), Schwer Murray Cap, also called continuous surface cap (MAT 145), CSCM Concrete (MAT 159), Mohr Coulomb (MAT 173), and Druker Prager (MAT 193) [3]. Category two generally employs the Prandtl–Reuss flow theory (where the Von Mises criterion is used as the plastic potential) to calculate the plastic strain increment. The plastic volume strain is obtained from the equations of state (EOS), and the plastic volume strain increment is independent of the incremental flow rule (the Prandtl–Reuss flow theory). Since shear and volumetric behaviors are decoupled, the phenomenon of shear dilation cannot be captured. Typical models belong to this category are the soil and form (MAT 5/14) [3], pseudo tensor (MAT 16) [3], concrete damage (MAT 72) [3,7], Winfrith concrete (MAT 84/85) [3,8], Johnson Holmquist concrete (MAT 111) [3,9], RHT (MAT 272) [3,10] and so on. Those models have been widely used to model concrete under high impact loads. The third category commonly assumes a non-associated flow in calculating the plastic strain increment. With a different plastic potential surface than the yield surface, the shear dilatancy can be well controlled. A typical example of this category is the plastic-damage model [5,11].

* Corresponding author at: Dept of Civil and Environmental Engineering, the Hong Kong University of Science and Technology, Clearwater Bay, Kowloon, Hong Kong SAR, China.
E-mail addresses: huajiang2006@hotmail.com (H. Jiang), jzhao@ust.hk (J. Zhao).

http://dx.doi.org/10.1016/j.finel.2014.12.002
0168-874X/

Notation

MAT 145 continuous surface (Schwer Murray) cap
MAT 159 CSCM concrete
MAT 72 concrete damage
MAT 72R3 concrete damage REL3 (K&C concrete)
MAT 25 geologic cap
MAT 111 Johnson Holmquist concrete
MAT 16 Pseudo tensor
MAT 272 RHT
MAT 84 Winfrith concrete
EOS equations of state
TXC triaixal compression
TOR torsion
TXE triaxial extension
CDM continuum damage mechanics
DERR damage energy release rate used by Simo and Ju [31]
RC reinforced concrete
I_1, J_2, J_3 three invariants of stress tensor
$R(I_1, J_3)$ Rubin scaling function in Eq. (1), used by Rubin [27]
κ, κ_0 cap hardening parameter in Eqs. (3) and (5)
$F_f(I_1)$, α, β, γ, θ strength in triaxial compression in Eqs. (1) and (2a)
Q_i, α_i, β_i, γ_i, $\theta_i (i=1,2)$ strength in torsion and triaxial extension in Eqs. (2b) and (2c)
$F_c(I_1, \kappa)$ the cap surface in Eqs. (1) and (3)
$X(\kappa)$, $L(\kappa)$, $X(\kappa_0)$ the cap surface parameters in Fig. 1.
S ratio of the major to minor axes of the cap surface in Eqs. (4), (18a), (18b) and (19e)
ε_v^p, W plastic volumetric strain and the maximum value in Eq. (6)
D_1, D_2 parameters determining the shape of pressure–volume in Eq. (6)
σ, $\bar{\sigma}$ stress tensor and effective stress tensor in Eq. (7)
$d, d^{\pm}$, $G(\bar{\tau}^{\pm})$ scalar damage variable in Eqs. (7) and (8)
$r_0^{\pm}$, $\bar{\tau}^{\pm}$ damage threshold and undamaged energy norm in Eq. (8)
f'_c, f'_{bc} uniaxial and biaxial compression strength of concrete
f'_t, f'_{bt} uniaxial and biaxial tension strength of concrete
τ_0, σ_0 shear strength and normal strength in Eq. (10), used by Mills and Zimmerman [20]
$g(\bar{\sigma}_{ij})$, $g(\bar{I}_1, \bar{J}_2)$ Gibbs free energy density (per unit volume) in Eqs. (22) and (24)
$g_1(\bar{J}_2)$, $g_2(\bar{I}_1)$ deviatoric and volumetric part of Gibbs free energy density in Eq. (22)
E, γ Yong's modulus and Poisson's ratio
K, G bulk modulus and shear modulus
D_{ijkl}^{-1} fourth-order linear-elastic compliance matrix tensor of the intact material in Eq. (21)
I_{ijkl}, I_{ijkl}^d fourth-order identity tensor and deviatoric tensor in Eq. (21)
G_F, G_{F0} the mode I fracture energy and base value of fracture energy per unit area in Eqs. (36)–(31)
σ(w), ω the stress and displacement in Eqs. (26)–(32)
G_c the compression fracture energy in Eqs. (32)–(36)
d_{max} the maximum aggregate size in Table 2
l^* a characteristic length of the finite element in Eqs. (29), (31), (35), (36)
$A^{\pm}$, $B^{\pm}$ damage parameters determining the strain softening curve in Eqs. (8) and (31), (36)
$\bar{\sigma}_{ij}$, $\tilde{\sigma}_{ij}$ the viscid and inviscid stress tensor in Eqs. (37)–(39)
η a fluidity coefficient parameter in Eqs. (37)–(39)

When concrete is subject to low velocity impact, there are typical features needing to be captured by a model, such as shear enhanced compaction, dilatency before and after peak strength, pre-peak hardening, post-peak softening, modulus reduction/stiffness degradation under cyclic loading, irreversible deformation, and localized damage accumulation [12,13]. With a sound theoretical basis, the MAT 145 available in LS-DYNA can well capture those behaviors together [3]. However, it has not been as popular as simple ones such as the MAT 72, MAT 84/85 and the MAT 111 in engineering application, due primarily to the complexity of the model with many material parameters involved. For example, a total of 17 material parameters is required to be provided by the user in this model to define the shear and cap surface, which demands exceedingly complicated experiments ranging from uniaxial compression, uniaxial tension, triaxial compression (TXC), torsion (TOR), triaxial extension (TXE) and hydrostatic test to be conducted for their calibration, which greatly limits the practical applicability of the model. On the other hand, a “sister” model-MAT 159 [3,14,15], with internal material parameters generation based upon the unconfined compression strength f'_c of concrete, aggregate size and the units has been included in LS-DYNA since version 971. This model uses the same methodology as the MAT 145 to predict the behavior of concrete before peak strength, and is different from the latter in terms of strain (post peak) softening portion for example the evolution of the both brittle damage and ductile damage norm. A comparison between the MAT 159 and MAT 145 will be provided in this research.

Indeed, similar issue exists for the MAT 72 which has a total of 49 user defined parameters. Karagozian & Case [16,17], Markovich et al. [18] managed to offer an approach of automatically

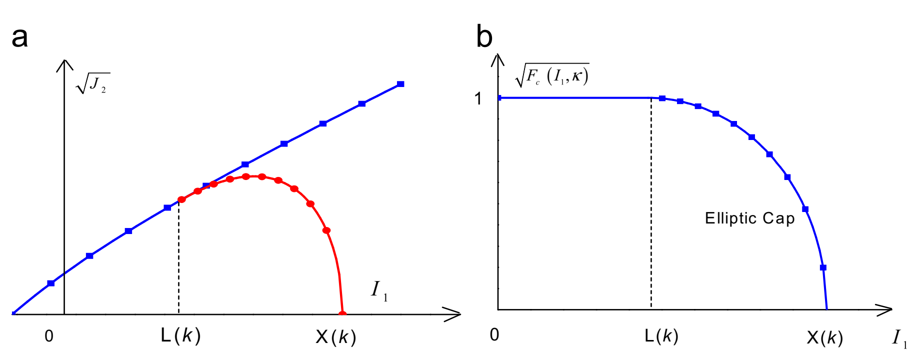

Fig. 1. Compressive meridional profile of the yield surface in the MAT 145: (a) smooth cap failure function, (b) non-dimensional function used for cap portion.